An improved asymptotic denoising algorithm for infrared images of electrical equipment based on Non-Local means

Yunlei Zhou, Xiaojie Dong*, Chengyi Liu, Minghuan Pi, Yanbo Le
College of Intelligent Systems Science and Engineering, Hubei Minzu University, Enshi 445000, China
*48553321@qq.com

ABSTRACT

Infrared images are susceptible to Gaussian noise during acquisition and transmission. To meet the quality requirements for infrared image data in image processing, an asymptotic Non-Local Means (NLM) algorithm based on an improved Scharr operator was proposed for denoising infrared images of electrical equipment. Firstly, the RGB infrared images were converted to the Y channel. Secondly, the improved Scharr operator was used to adjust the computation weights of the NLM algorithm, better preserving the edge details of the images. To optimize the denoising effect, a multi-layer pyramid was constructed, and a layer-by-layer denoising fusion method was adopted to obtain the initially denoised images. Finally, for the residual noise in the initially denoised images, asymptotic denoising was employed, adjusting the filter parameters based on the image characteristics for secondary denoising, followed by image reconstruction to obtain the denoised images. Experimental results showed that the proposed algorithm achieved clear and complete denoised images, with Peak Signal-to-Noise Ratio (PSNR) and Structural Similarity (SSIM) improved by 0.78 to 4.95 and 0.01 to 0.08, respectively, compared to other methods. This indicated that the method is effective for high-efficiency denoising of infrared images of electrical equipment.

Keywords: Infrared image, Gaussian noise, Non-Local means algorithm, Scharr operator, Multi-layer pyramid, Asymptotic denoising

1. INTRODUCTION

The normal operation of electrical equipment is crucial, and infrared detection technology plays a key role in fault detection due to its non-contact nature, speed, and accuracy. By using infrared thermal imaging, staff can analyze the temperature distribution of the equipment and assess its operational status, making it an essential tool for monitoring electrical equipment[1]. In the context of big data, computer vision technologies such as object detection and image segmentation are widely applied in the electrical field. However, during the acquisition and transmission of infrared images, they are primarily affected by Gaussian noise, which can interfere with image processing. Therefore, image denoising is a critical step to ensure the accuracy of image analysis.

In early denoising research, Buades et al.[2] proposed the NLM algorithm, which leverages the self-similar characteristics of images. By considering the similarity between local information and applying weighted averaging, it achieves good results. However, the algorithm does not account for image edges or details, leading to issues like blurred edges and lost details. To address these issues, Guo Chenlong et al.[3] proposed a gradient-based structural similarity algorithm (GSSIM) to improve the NLM algorithm. This method effectively preserves the details and edges of the image while removing Gaussian white noise from infrared images, thereby mitigating the blurring and distortion problems caused by traditional methods. In order to better remove Gaussian noise, KANG Kai et al.[4] combined steering kernel regression and guided image filtering, optimizing filtering weights to remove Gaussian noise while preserving image edges and details. Most denoising methods first convert infrared images of electrical equipment to grayscale, which cannot be restored to color infrared images. For tasks like target detection, where color is crucial for identifying thermal fault points, it is important to enhance denoising in RGB infrared images. This paper proposes a progressive non-local means denoising algorithm using an improved Scharr operator to efficiently denoise while preserving edge details. The denoised Y-channel image is combined with the Cb and Cr channels to reconstruct the RGB infrared image, aiding tasks such as target detection and adding practical value.

International Conference on Network Communication and Information Security (ICNCIS 2024),
edited by Ljiljana Trajkovic, Pascal Lorenz, Proc. of SPIE Vol. 13516, 135160N
 · 0277-786X · doi: 10.1117/12.3051999

2. FUNDAMENTAL PRINCIPLE OF THE NLM

Assuming a normal infrared image is corrupted by Gaussian noise, its observation model can be described as:

$$f(i,j) = g(i,j) + n(i,j) \tag{1}$$

Where, $f(i,j)$ represents the image with Gaussian noise; $g(i,j)$ represents the noise-free true image; $n(i,j)$ denotes the noise value at a pixel point, which in this paper is Gaussian noise with a mean of 0 and variance σ^2.

For the noisy image $f(i,j)$ in Equation (1), the denoised value $\hat{f}(i,j)$ at each pixel (i,j), calculated as the weighted average of its neighboring pixels (k,l) using the NLM algorithm, can be expressed as:

$$\hat{f}(i,j) = \sum_{(k,l)\in\Omega} \frac{\omega((i,j),(k,l))}{\sum_{(k,l)\in\Omega} \omega((i,j),(k,l))} f(k,l) \tag{2}$$

$$\omega((i,j),(k,l)) = \exp\left(-\frac{d((i,j),(k,l))}{h^2}\right) \tag{3}$$

$$d((i,j),(k,l)) = \| N(i,j) - N(k,l) \|_{2,a}^2 = \| G_a \otimes [N(i,j) - N(k,l)] \|_2^2 \tag{4}$$

Where, $N(i,j)$ and $N(k,l)$ represent the local patches centered at pixel points (i,j) and (k,l), respectively; G_a is a Gaussian kernel matrix with a standard deviation of a, and $\otimes$ denotes element-wise multiplication within the matrix. $\omega((i,j),(k,l))$ represents the weight between $N(i,j)$ and $N(k,l)$, reflecting their similarity. As shown in Equation (3), a larger weighted Euclidean distance results in a smaller weight, indicating lower similarity, and vice versa. h controls the decay rate and is proportional to the noise intensity. The algorithm compares the local patch with each similar patch in the search neighborhood Ω, which theoretically could be the entire image but is typically limited to a local region of size $q \times q$ for practical reasons.

3. EDGE-DETECTION-BASED IMPROVED NLM ALGORITHM

The edge-detection-based NLM algorithm aims to preserve edge details while removing noise. Common edge detection operators include Sobel, Scharr, and Prewitt. The Scharr operator offers clearer and more accurate results than Sobel and Prewitt, making it suitable for high-detail image applications. Thus, this paper uses the Scharr operator for edge detection.

3.1 Improved scharr operator

The Scharr operator highlights image edges by calculating the gradient at each pixel in the horizontal and vertical directions, using two 3x3 convolution kernels, as shown in Figure 1. These kernels are used to perform convolution operations in the horizontal and vertical directions, respectively, to obtain the gradient values in each direction. Finally, by combining the gradient values from these two directions, the edge positions and orientations in the image can be determined. To address the directional limitations and limited precision of the traditional Scharr operator, this paper introduces improvements in two aspects: gradient enhancement and threshold selection.

3	0	−3
10	0	−10
3	0	−3

(a)Horizontal direction template.

3	10	3
0	0	0
−3	−10	−3

(b)Vertical direction template.

Figure 1. Traditional Scharr operator template.

3.1.1Scharr operator gradient enhancement

Assume there is a 3x3 Y-channel image patch, where the grayscale value of pixel (i, j) is denoted by $g(i, j)$ .To enhance the Scharr operator's sensitivity to grayscale variations in other directions, the improved Scharr operator in this paper adds two additional directions, 45 degrees and 135 degrees, compared to the traditional Scharr operator. The corresponding templates are shown in Figure 2.

3	0	−3
10	0	−10
3	0	−3

(a)0 degrees.

10	3	0
3	0	−3
0	−3	−10

(b)45 degrees.

3	10	3
0	0	0
−3	−10	−3

(c)90 degrees.

0	3	10
−3	0	3
−10	−3	0

(d)135 degrees.

Figure 2. Four-direction convolution template.

Using the four-direction Scharr operator to traverse each pixel in the image, The convolution calculation formula is as follows:

$$G_n(i, j) = \sum_{m=-1}^{1} \sum_{n=-1}^{1} G_n(m, n) \cdot g(i+m, j+n) \tag{5}$$

For each pixel, the weighted gradient results in the four directions are calculated, and the maximum value is taken as the gradient value of that pixel. The direction of the template corresponding to this maximum value is the edge direction of the pixel. Finally, the gradient magnitude image $G(i, j)$ of $g(i, j)$ is obtained. The gradient value of any pixel is expressed as follows:

$$\nabla g(i, j) = \max\left\{G_0, G_{45}, G_{90}, G_{135}\right\} \tag{6}$$

3.1.2 Threshold selection

Although the improved Scharr operator can provide more complete edge information, threshold selection remains crucial. If the threshold is set too high, edges and details will be lost; if the threshold is set too low, noise will be amplified, leading to an increase in false edges, which affects the accuracy of the detection results and the integrity of the image contours. The traditional Scharr operator determines the threshold through multiple experiments and binarizes the gradient magnitude image. To overcome this issue, this paper adopts the mean adaptive thresholding method, setting appropriate thresholds for different regions of the image:

1) Define the local window: Define a local window for each pixel to calculate the average value of the pixels within that region. The window size is selected based on the characteristics of the image and the noise level.
2) Calculate the local average: Calculate the average grayscale value of the pixels within the window centered on each pixel, representing the local features.
3) Calculate the adaptive threshold: Subtract a constant C from the computed local average to obtain the adaptive threshold for that window. The constant is adjusted based on the noise level of the image, set to 5 for high-noise scenarios and 2 for low-noise scenarios.
4) Apply thresholding. Compare the gradient intensity with the adaptive threshold to determine the edge image:

$$E(i, j) = \begin{cases} 1, & G(i, j) > T(i, j) \\ 0, & G(i, j) \le T(i, j) \end{cases} \tag{7}$$

(a)Original image of the current transformer Y channel.

(b)Traditional Scharr operator edge detection.

(c)Improved Scharr operator for edge detection.

Figure 3. Detection of edges in current transformers using two edge detection operators.

As shown in Figure 3, the improved Scharr operator has a stronger ability to preserve image details compared to the traditional Scharr operator. The former provides more complete edge information, smoother curves, and can fully display the contour information of electrical equipment such as current transformers.

3.2 Weight function based on the improved Scharr operator

In the traditional NLM algorithm, the weights rely solely on the similarity of pixel blocks, which can easily result in blurred edges and loss of details, especially when there are significant brightness differences within the neighborhood blocks. In such cases, the similarity measurement may be inaccurate, leading to artifacts and distortion. Additionally, the NLM algorithm lacks adaptability when processing smooth regions and detail-rich regions. Therefore, this paper introduces edge detection using the four-direction Scharr operator to obtain an edge strength image E, which is incorporated into the weight calculation of the NLM algorithm. The modified weight function, as shown in Equation (8), allows for better preservation of image details and edge information.

$$\omega((i,j),(k,l)) = \exp(-\frac{d((i,j),(k,l))}{h^2}) \bullet \exp(-\alpha E(k,l)) \tag{8}$$

Where, $E(k,l)$ serves as a weight adjustment factor and takes a value of either 0 or 1. Let $\omega_e = \exp(-\alpha E(k,l))$. Here, α is an adjustment coefficient that can control the influence of edge pixels. In this paper, $\alpha = 0.1$.

According to the modified weight function, for edge regions in the image, when $E(k,l) = 1$, the value of ω_e approaches 0, reducing the weight of edge pixels and thereby decreasing the smoothing effect in edge areas, which helps preserve edge sharpness. For non-edge regions in the image, when $E(k,l) = 0$, the value of ω_e is 1, so the weight is entirely determined by the similarity of the pixel blocks. This approach minimizes the influence on complex texture regions. This algorithm is named SNLM in this paper.

3.3Multiscale pyramid optimization for denoising

The purpose of constructing a multi-layer pyramid is to handle noise at different scales within the image[5], thereby optimizing the denoising effect. The steps are as follows:

1) Construct a multi-layer pyramid: Build a multi-layer pyramid structure through Gaussian blurring and downsampling, where layer 0 is the high-resolution original image, and the resolution decreases progressively in each subsequent layer.

2) Progressive denoising: Perform denoising at different levels of the pyramid. Starting from the lowest resolution layer, the improved SNLM algorithm is applied progressively to higher resolution layers to obtain the denoised image.

3) Progressive upsampling and fusion: Upsample the denoised image, fuse it with the previous layer's original image, and repeat until the original resolution is restored. The final denoised image I is obtained from Equation (9).

$$I = \beta \hat{I}_n + (1-\beta) I_u \tag{9}$$

Where, I is the final image, $\hat{I}_n$ is the denoised image at the current layer, I_u is the upsampled image, and β is the fusion weight, which is set to 0.5 in this paper.

3.4Algorithm flow of this paper

Considering that in the NLM algorithm, when the filter parameter h is set to a larger value, a significant amount of noise can be removed, resulting in a smoother image, but this may cause blurring of image details; when the filter parameter h is set to a smaller value, details can be better preserved. Therefore, this paper adopts a progressive denoising approach. In the first denoising step, the multi-scale pyramid optimized SNLM algorithm is used with $h_1 = 1.1\sigma$; in the second denoising step, the SNLM algorithm is directly applied to the result of the first denoising, with $h_2 = 0.8h_1$ .The overall algorithm flowchart is shown in Figure 4.

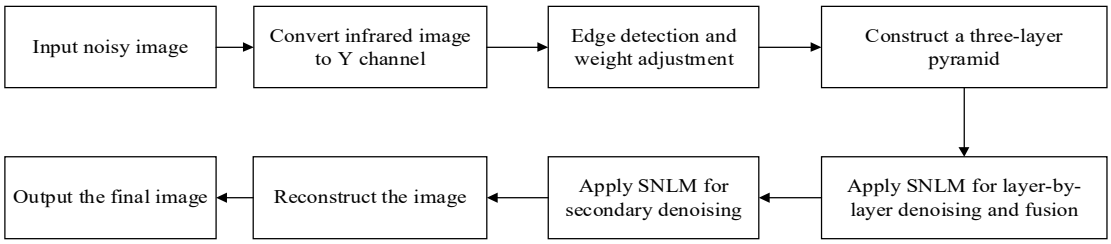

Figure 4. The overall algorithm flowchart.

4. EXPERIMENTAL ANALYSIS

To verify the effectiveness of the improved method proposed in this paper, actual infrared images of electrical equipment from the Roboflow website were selected for algorithm validation. Noisy infrared images were created by adding Gaussian noise of varying intensities, followed by noise removal. The denoising results were then compared with the NLM algorithm, Block-Matching and 3D Filtering (BM3D) [6], Perona-Malik nonlinear diffusion denoising algorithm (P-M) [7], and the NLM algorithm based on the improved Scharr operator (SNLM).

4.1Evaluation metrics

To objectively evaluate and compare the noise removal effectiveness of the proposed algorithm, PSNR and SSIM are used as evaluation metrics to quantitatively analyze the performance of different denoising methods. PSNR assesses image quality based on pixel differences, while SSIM evaluates image similarity by considering luminance, contrast, and structural information. The specific formulas are shown in Equations (10) and (11):

$$\begin{cases} PSNR = 10\lg\dfrac{(f_{\max} - f_{\min})^2}{MSE} \\ MSE = \dfrac{1}{N}\sum_{i=1}^{N}\left[u(i) - \hat{u}(i)\right]^2 \end{cases} \tag{10}$$

Where, $f_{\max}$ and $f_{\min}$ represent the maximum and minimum pixel values of the image; $u(i)$ and $\hat{u}(i)$ represent the grayscale values of the original image and the denoised image at pixel i ; N denotes the number of pixels in the image.

$$\begin{cases} SSIM(x,y) = l(x,y)c(x,y)s(x,y) \\ l(x,y) = \dfrac{2\mu_x\mu_y + C_1}{\mu_x^{\,2} + \mu_y^{\,2} + C_1} \\ c(x,y) = \dfrac{2\sigma_x\sigma_y + C_2}{\sigma_x^{\,2} + \sigma_y^{\,2} + C_2} \\ s(x,y) = \dfrac{\sigma_{xy} + C_3}{\sigma_x\sigma_y + C_3} \end{cases} \tag{11}$$

Where, $l(x,y)$, $c(x,y)$, and $s(x,y)$ represent luminance comparison, contrast comparison, and structure comparison, respectively; μ_x and μ_y are the mean values of images x and y, respectively; σ_x and σ_y are their standard deviations; σ_{xy} is the covariance between them; C_1, C_2, and C_3 are constants.

4.2Experimental verification

In this paper, 10 infrared images of various electrical equipment were used for denoising simulation, labeled 1-10. Gaussian noise with intensities of 10, 20, and 30 was added to the original images to create noisy images. The proposed algorithm was tested for denoising each image at different noise levels and compared with NLM, BM3D, P-M, and SNLM algorithms. The PSNR and SSIM results for the proposed and comparison algorithms are presented in Table 1. Specifically, Figure 5 shows the denoising results of a current transformer image with moderate Gaussian noise (mean 0, standard deviation 20) using different methods.

Table 1. Average denoising test results at different noise intensities.

Noise Intensity	P-M		BM3D		NLM		SNLM		Ours	
	PSNR	SSIM	PSNR	SSIM	PSNR	SSIM	PSNR	SSIM	PSNR	SSIM
$\sigma=10$	35.21	0.946	34.09	0.956	29.08	0.903	36.80	0.959	**37.84**	**0.971**
$\sigma=20$	30.99	0.877	31.58	0.939	28.84	0.889	32.71	0.921	**33.36**	**0.948**
$\sigma=30$	27.94	0.773	28.66	0.905	28.38	0.863	29.30	0.882	**29.95**	**0.921**

From a visual perspective, the denoised images produced by the comparison methods exhibit issues such as noise residue and blurred edges and details. In contrast, the results from the proposed algorithm are much closer to the original image, demonstrating superior noise removal and detail preservation capabilities compared to the other methods. Furthermore, as shown in Table 1, based on the image denoising performance metrics, the proposed algorithm outperforms the comparison methods under different noise intensities. The average PSNR results show an improvement of 2.34, 2.27, 4.95, and 0.78 compared to the other methods, while the average SSIM results show improvements of 0.08, 0.01, 0.06, and 0.02.

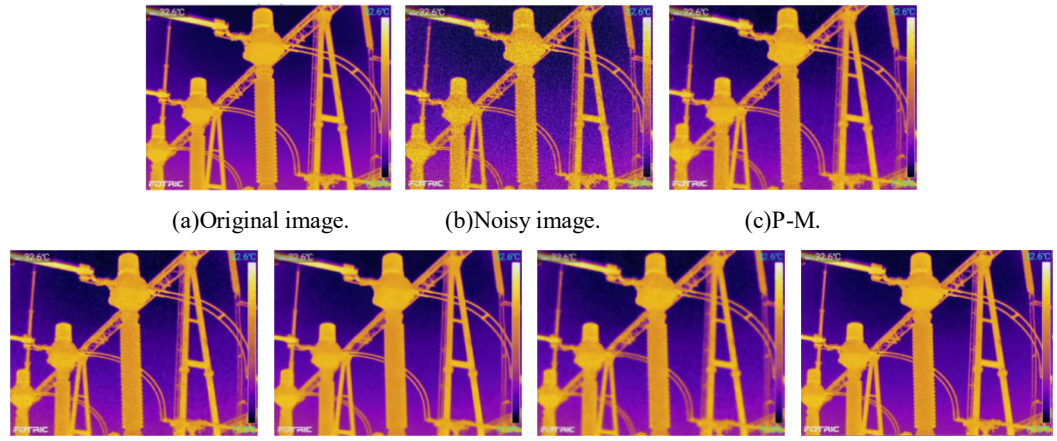

(a)Original image. (b)Noisy image. (c)P-M.

(d)BM3D. (e)NLM. (f)SNLM. (g)Ours.

Figure 5. Comparison of denoising algorithms for infrared images of current transformers.

5. CONCLUSION

An improved Scharr operator-based progressive NLM algorithm was proposed for denoising RGB infrared images of electrical equipment. The main work includes the following three points:

1) Improved the NLM weight function: By refining the Scharr operator and adopting a new threshold selection method, more complete and clearer edge images were obtained, which optimized the NLM weight function and enhanced the denoising effect and edge preservation capability of RGB infrared images.

2) Used a multi-layer pyramid structure: By applying multi-layer pyramid denoising, the denoising effect was significantly improved.

3) Adjusted filter parameters: By tuning the secondary filtering parameters based on image characteristics, residual noise in the image was significantly reduced, and more edge details were preserved.

Although the algorithm presented in this paper has achieved certain results, the use of multi-layer pyramid and progressive denoising methods leads to higher computational complexity, which may affect processing speed. The next step is to improve its runtime while maintaining effectiveness, potentially by using GPU parallel computation to accelerate the process. Additionally, while the algorithm performs excellently in denoising infrared images of electrical equipment, its applicability to mixed noise and other types of images still requires further validation and research.

REFERENCES

[1] Shanmugam C, Chandira E S, Sivakumar A, et al. Fault Detection in Electrical Equipment by Infrared Thermography Images Using Spiking Neural Network Through Hybrid Feature Selection [J]. Journal of Circuits, Systems and Computers, 2023, 32(08):

[2] Buades A, Coll B, Morel J. A Review of Image Denoising Algorithms, with a New One. [J]. Multiscale Modeling & Simulation, 2005, 4(2): 490-530.

[3] Guo Chenlong, Zhao Xuyang, Zheng Haiyan, et al. An Improved Non-Local Means Filtering Algorithm for Infrared Image Denoising. Infrared Technology, 2018, 40(07): 638-641.

[4] KAI Kang, TINGTING Liu, XIANCHUN Xu, et al. Study of infrared image denoising algorithm based on steering kernel regression image guided filter[C]//2019 18th International Conference on Optical Communications and Networks (ICOCN). Huangshan, China: IEEE, 2019: 1-3.

[5] Panpan H, Lanxue D. A multi-scale pyramid feature fusion-based object detection method for remote sensing images [J]. International Journal of Remote Sensing, 2023, 44(24):7790-7807.

[6] Kostadin D, Alessandro F, Vladimir K, et al. Image denoising by sparse 3-D transform-domain collaborative filtering. [J]. IEEE transactions on image processing: a publication of the IEEE Signal Processing Society, 2007, 16(8): 2080-95.

[7] Yıldırım A, Karaca İ. A PDE-based Mathematical Method in Image Processing: Digital-Discrete Method for Perona-Malik Equation [J]. American Academic Scientific Research Journal for Engineering, Technology, and Sciences, 2021, 84(1):118-129.